J. Cell. Mol. Med. Vol 16, No 11, 2012 pp. 2620-2630

Senescence determines the fate of activated rat pancreatic stellate cells

Brit Fitzner [a], Sarah Müller [a], Michael Walther [a], Madlen Fischer [a], Robby Engelmann [b], Brigitte Müller-Hilke [b], Brigitte M. Pützer [c], Michael Kreutzer [b, d], Horst Nizze [e], Robert Jaster [a, *]

[a] *Department of Medicine II, Division of Gastroenterology, University of Rostock, Rostock, Germany*
[b] *Institute of Immunology, University of Rostock, Rostock, Germany*
[c] *Department of Vectorology and Experimental Gene Therapy, University of Rostock, Rostock, Germany*
[d] *Center of Medical Research, University of Rostock, Rostock, Germany*
[e] *Institute of Pathology, Medical Faculty, University of Rostock, Rostock, Germany*

Received: January 23, 2012; Accepted: March 21, 2012

Abstract

In chronic pancreatitis (CP), persistent activation of pancreatic stellate cells (PSC) converts wound healing into a pathological process resulting in organ fibrosis. Here, we have analysed senescence as a novel mechanism involved in the termination of PSC activation and tissue repair. PSC senescence was first studied *in vitro* by establishing long-term cultures and by applying chemical triggers, using senescence-associated β-Galactosidase (SA β-Gal) as a surrogate marker. Subsequently, susceptibility of PSC to immune cell-mediated cytolysis was investigated employing cocultures. Using the model of dibutyltin dichloride-induced CP in rats, appearance of senescent cells was monitored by immunohistochemistry and immunofluorescence, and correlated with the progression of tissue damage and repair, immune cell infiltration and fibrosis. The results indicated that long-term culture and exposure of PSC to stressors (doxorubicin, H_2O_2 and staurosporine) induced senescence. Senescent PSC highly expressed CDKN1A/p21, mdm2 and interleukin (IL)-6, but displayed low levels of α-smooth muscle actin. Senescence increased the susceptibility of PSC to cytolysis. In CP, the number of senescent cells correlated with the severity of inflammation and the extension of fibrosis. Areas staining positive for SA β-Gal overlapped with regions of fibrosis and dense infiltrates of immune cells. Furthermore, a close physical proximity of immune cells and activated PSC was observed. We conclude that inflammation, PSC activation and cellular senescence are timely coupled processes which take place in the same microenvironment of the inflamed pancreas. Lymphocytes may play a dual-specific role in pancreatic fibrogenesis, triggering both the initiation of wound healing by activating PSC, and its completion by killing senescent stellate cells.

Keywords: chronic pancreatitis • fibrosis • cellular ageing

Introduction

Pancreatic stellate cells play a key role in fibrogenesis associated with CP and pancreatic cancer (PC). Profibrogenic stimuli such as ethanol metabolites, oxidative stress and various cytokines induce a process termed PSC activation. Activated PSC proliferate at a high rate, express the myofibroblast marker α-smooth muscle actin (α-SMA), secrete large amounts of extracellular matrix proteins, but lack the Vitamin A-containing fat droplets of quiescent PSC [1, 2]. PSC activation represents a wound healing response after pancreatic injury and is not pathological per se. Repeated episodes of tissue damage (CP) and continuous stimulation of PSC with profibrogenic stimuli (PC), however, may lead to persistent PSC activation and pancreatic fibrosis, which has been implicated in the development of organ failure in CP and progression of PC [1, 2]. Along these lines, triggering termination of the wound healing response might be a more promising approach to an antifibrotic treatment than inhibition of PSC activation itself.

Currently, it is largely unknown how precisely pancreatic fibrogenesis is terminated. Two principal mechanisms that have been proposed are the return to a quiescent phenotype, and elimination of activated PSC by apoptosis. Re-induction of quiescence has been observed *in vitro* and most recently also *in vivo* in response to Vitamin A [3, 4]. The contribution of this process to the termination of wound healing after pancreatic injury, however, remains to be shown.

*Correspondence to: Robert JASTER, M.D.,
Department of Medicine II, Division of Gastroenterology, University of Rostock, E.-Heydemann-Str. 6, D-18057 Rostock, Germany
Tel.: +49 381 494 7349
Fax: +49 381 494 7482
E-mail: jaster@med.uni-rostock.de

doi: 10.1111/j.1582-4934.2012.01573.x

Apoptosis of PSC, on the other hand, has been verified in various studies [5–8], but is poorly understood with respect to its specific prerequisites in the context of pancreatic disorders.

Herein, we have investigated the involvement of a third, primary independent process in the termination of PSC activation and wound healing: cellular senescence. To the best of our knowledge, senescence of stellate cells in the pancreas has not been shown before. Studies in the field of liver fibrosis, however, have suggested that senescence of activated hepatic stellate cells (HSC) strongly facilitates their subsequent elimination by natural killer (NK) cells, and shown a major role of this process in the resolution of fibrosis [9]. The senescence programme has therefore been implicated in the limitation of the fibrogenic response to acute tissue damage [9, 10].

Cellular senescence is defined as an irreversible form of cell cycle arrest. It may limit the proliferative potential of premalignant cells, and represents an important barrier mechanism against tumourigenesis [11]. Originally linked to replicative exhaustion (caused by telomere shortage), cellular senescence has later on also been shown to be triggered by diverse forms of cellular damage or stress. Thus, some anticancer drugs (*e.g.* doxorubicin) exert their cytostatic effects, at least in part, through the induction of senescence [9–11]. Senescent cells are usually characterized by the accumulation of a senescence-associated β-galactosidase (SA β-Gal) activity that distinguishes them from most quiescent cells. Although SA β-Gal activity is considered the gold standard, many other surrogate markers for cellular senescence have been proposed as well, such as a flattened morphology, presence of senescence-associated heterochromatin foci, activation of the tumour suppressor pathways p53 and p16/Rb and a characteristic gene expression profile with high levels of cell cycle inhibitors; *e.g.* CDKN1A/p21 [11]. Many senescent cells, including HSC, also exhibit a so-called senescence-associated secretory phenotype: they overexpress genes encoding secreted proteins that can alter the tissue microenvironment [9–11].

We started our investigation with *in vitro* studies on mechanisms and consequences of PSC senescence. Using the model of dibutyltin dichloride (DBTC)-induced CP in rats [12], we then also analysed the involvement of cellular senescence in pancreatic wound healing under *in vivo* conditions. Together, our data suggest a previously unrecognized role of cellular senescence in the regulation of pancreatic fibrogenesis.

Materials and methods

Cell isolation and culture

Quiescent PSC were isolated by collagenase digestion of the pancreas followed by Nycodenz density gradient centrifugation as previously described [13]. PSC were cultured in IMDM supplemented with 17% foetal calf serum, 1% non-essential amino acids (dilution of a 100X stock solution), 100 U/ml penicillin and 100 μg/ml streptomycin at 37° C in a 5% CO_2 humidified atmosphere. The cells were grown on culture plates to subconfluency, harvested by trypsination and recultured at equal seeding densities. Most experiments were performed with cells termed young PSC that were recultured only once. In some studies, cell cultures of passage 5 or more, defined as old PSC, were used. In case of multiple passages, the cells were seeded at a density of 50,000 cells per well of a six-well plate and recultured once per week. If the cells were exposed to growth-inhibitory agents, the seeding density was increased according to the specific experimental requirements, avoiding, however, cell confluency in the course of the study.

Splenocytes were isolated from the spleen of healthy rats using a cell strainer (70 μm). Red blood cells were lysed applying NH_4Cl (0.25 M) lysing solution. After centrifugation, the cell pellet was resuspended in PBS with 0.1% FCS and in case of isolating NK cells subjected to Magnetic Activated Cell Sorting (MACS). Rat NK cells were separated in an autoMACS Separator (Miltenyi Biotec GmbH, Bergisch Gladbach, Germany) by a negative selection for CD3 and positive selection for CD161, using R-phycoerythrin (PE)-labelled anti-CD3 and FITC-labelled anti-CD161 antibodies (Immunotools, Friesoythe, Germany). Isolation was performed following standard methods and suggestions of the manufacturer. The purity of $CD3^-$, $CD161^+$-cells was verified by FACS analysis (FACSCalibur cytometer; BD Biosciences, Heidelberg, Germany) and always reached at least 93%.

For direct coculture studies, PSC pre-treated as indicated were harvested by trypsination and labelled with carboxyfluorescein succinimidyl ester (CFSE; application at 1 μM for 20 min.). PSC and freshly isolated NK cells were seeded together at a ratio of 1:20 into culture plates. After an incubation period of 16 hrs, PSC and NK cells were harvested and subjected together to FACS analysis. Immediately before measurement, propidium iodide (PI) was added at 200 μg/ml. Dead PSC were defined as CFSE and PI double-positive cells.

All experiments were performed in the presence of serum. When the cells were exposed to drugs such as triggers of senescence, the substances were replenished every 2–3 days. All substances, except of H_2O_2, were dissolved in DMSO. The final DMSO concentration did not exceed 0.2% and displayed no effects in solvent control experiments.

Quantification of DNA synthesis

Cell proliferation was assessed using a 5-bromo-2′-deoxyuridine (BrdU) labelling and detection enzyme-linked immunosorbent assay kit (Roche, Mannheim, Germany). Therefore, PSC were seeded at equal densities into 96-well plates in the presence of drugs as indicated. Twenty-four hours later, BrdU labelling was initiated by adding labelling solution at a final concentration of 10 μM to the culture medium. After an overnight incubation, labelling was stopped and BrdU uptake was measured according to the manufacturer's instructions.

Analysis of telomeres

Telomere length was assessed using the Telomere peptide nucleic acid (PNA) Kit/fluorescein isothiocyanate (FITC) for flow cytometry according to the instructions of the manufacturer (Biozol, Eching, Germany). Briefly, cellular DNA was denatured for 10 min. at 82°C, before it was hybridized with the fluorescein-conjugated PNA probe in the dark at room temperature overnight. After several washing steps, the samples were incubated with DNA staining solution for identification of $G_{0/1}$ cells, and subjected to flow cytometric analysis. The data were expressed as relative telomere length, using the cell line 1301 as a standard for very long telomeres. Therefore, the ratio between the telomere signal of stellate cells and 1301 cells (with correction for the DNA index of $G_{0/1}$ cells) was calculated.

Experimental pancreatitis

Male Lewis rats were kept under standard laboratory conditions and fed a rodent chow diet. All experiments were performed according to the guidelines of the local animal use and care committee. Experimental chronic pancreatitis was induced by the injection of DBTC at the indicated dose into the tail vein as described before [12, 14]. At various time-points after DBTC injection (1, 2, 4 and 8 weeks respectively), rats were killed under anaesthesia by overdosing pentobarbital. The pancreas was removed, and tissue samples were subjected to histological analysis.

To study the role of NK cells, rats were depleted of these cells prior to the induction of DBTC-pancreatitis by five intraperitoneal injections (one every third day) of anti-CD161 antibodies (100 μg per injection). Control rats received equal amounts of a non-specific IgG (Intratect; Biotest Pharma, Dreieich, Germany). After initiation of pancreatitis (application of 6 mg/kg DBTC), depletion of NK cells was maintained by weekly injections of 100 μg anti-CD161 antibodies. The rats were killed on day 28 after DBTC injection.

Histology and immunohistochemistry

Paraffin-embedded pancreatic sections were stained according to standard protocols using haematoxylin and eosin (H&E). Pathological changes of parenchyma (acini and ducts), interstitial space (oedema, cellular infiltration and periductal/interstitial fibrosis), fatty tissue and Langerhans islets were graded on a semi-quantitative scale from 0 (none) to 3 (severe), using a scoring system as previously described [15, 16]. Inflammatory cells, expression of α-SMA and desmin were further classified by immunohistochemical analysis, employing cryostat tissue sections and the alkaline phosphatase anti-alkaline phosphatase (APAAP) technique. In detail, 6-μm-thick cryostat sections of pancreatic tissue were incubated sequentially with unlabelled primary mouse monoclonal antibody, rabbit antimouse IgG (Dako, Glostrup, Denmark) and monoclonal mouse APAAP complex (Dako). Alkaline phosphatase activity was visualized using the fuchsin^{+} substrate-chromogen system and levamisole according to the instructions of the manufacturer (Dako). Cell nuclei were counterstained with Mayer's haematoxylin and mounted in Aquatex (Merck, Darmstadt, Germany).

In case of α-SMA detection, precise counting of the cells was hampered by the extensive staining of large tissue areas in some samples. Therefore, a semi-quantitative scoring was performed (score 0: $\leq$5%, 1: 6–15%, 2:16–25%, 3: >25% red-stained tissue). All samples were blinded prior to evaluation.

Indirect immunofluorescence staining

For indirect immunofluorescence staining, 6-μm-thick cryostat tissue sections of pancreatic tissue were fixed with acetone for 10 min. In case of cell culture studies, the cells were grown on glass cover slips and fixed with methanol. Non-specific binding sites were blocked with 1% bovine serum albumin (in PBS with 0.1% Tween 20; PBS-T) for 30 min. Subsequently, the respective primary antibody (diluted in PBS-T) was added for 1 hr. Antibody binding was detected by incubation for 1 hr with the secondary immunoglobulins, directed against the species of the primary antibody, AlexaFluor 488 (green) and AlexaFluor 546 (red; Invitrogen, Karlsruhe, Germany) respectively. For double staining, the procedure was repeated with another suitable combination of primary and secondary antibodies. Nuclei were visualized by counterstaining with 4′,6-Diamidino-2-phenylindole (DAPI). Analysis of fluorescence was performed using an AxioScope.A1 (Carl Zeiss MicroImaging GmbH, Jena, Germany).

Detection of SA β-Gal

The SA β-Gal in cells cultured on cover slips and in 6-μm-thick cryostat tissue sections was stained using a specific staining kit (New England BioLabs, Frankfurt, Germany). Unless indicated otherwise, the nuclei of cultured cells were counterstained with DAPI according to standard protocols. Subsequently, specimens were analysed by light and fluorescence microscopy. Image evaluation was performed using an ImageMagick-based software to distinguish between SA β-Gal-positive and negative cells.

Tissue sections (and cell cultures, if indicated) were counterstained with nuclear fast red. For semi-quantitative analysis, the following scoring system was employed: 0: complete/almost complete absence of SA β-Gal-positive cells, 1: scattered SA β-Gal-positive cells (less than 5% of the sample), 2: 5–25% SA β-Gal-positive cells, 3: SA β-Gal-positive areas covering more than 25% of the section.

All samples were evaluated in a blinded manner.

Quantification of interleukin-6 protein

Interleukin-6 in cell culture supernatants was quantified using an ELISA kit for the rat protein (R&D Systems, Minneapolis, MN, USA). Therefore, the cells were exposed to drugs for 7 days as indicated. The cell culture supernatants, received after a collection period of 96 hrs, were stored at −80°C until they were assayed. IL-6 levels were normalized by relating them to the cell counts obtained on day 7 by trypan blue staining.

Quantitative reverse transcriptase using real-time TaqMan™ technology

Total RNA from PSC pre-treated as indicated was isolated with peqGOLD TriFast reagent (Peqlab Biotechnologie, Erlangen, Germany) according to the manufacturer's instructions. Following DNAse digestion of genomic DNA, RNA was reverse transcribed into cDNA by means of TaqMan™ Reverse Transcription Reagents (Applied Biosystems, Foster City, CA, USA) and random hexamer priming. Relative quantification of target cDNA levels by real-time PCR was performed in an ABI Prism 7000 sequence detection system using TaqMan™ Universal PCR Master Mix and the following Assay-on-Demand™ rat gene-specific fluorescently labelled TaqMan™ MGB probes (Applied Biosystems): Rn00561420_m1 (IL-6), Rn01759928_g1 (α-SMA; acta2), Rn00589996_m1 (CDKN1A/p21), Rn03399818_s1 (mdm2), Rn00755717 (p53) and Rn01527840_m1 (HPRT). PCR was performed under the following conditions: 95°C for 10 min., 50 cycles of 15 sec. at 95°C, 1 min. at 60°C. Relative expression of each mRNA compared with the housekeeping gene HPRT was calculated according to the equation $\Delta Ct = Ct_{target} - Ct_{HPRT}$. The relative amount of target mRNA in control cells and cells treated as indicated was expressed as $2^{-(\Delta\Delta Ct)}$, where $\Delta\Delta Ct_{treatment} = \Delta Ct_{sample} - \Delta Ct_{control}$. The reactions were performed in triplicate, and repeated at least six times with independent samples.

Statistical analysis

Results are expressed as mean ± S.E.M. for the indicated number of separate cultures, tissues or rats per experimental protocol. Statistical significance was analysed using the Wilcoxon rank sum test. $P < 0.05$ was considered to be statistically significant.

Results

Long-term culture and chemical triggers induce PSC senescence

The PSC of passage 1 (subsequently termed young PSC) stained weakly positive for α-SMA and displayed the typical morphology of early activated PSC, as indicated by the immunofluorescent staining of the cytoskeleton protein β-actin (Fig. 1A, left upper and middle panel). Young PSC did not express detectable amounts of SA β-Gal (left lower panel). After six passages, many PSC stained strongly positive for α-SMA, and showed an increased size and a flat morphology (right upper and middle panel). These old PSC also expressed at a high rate SA β-Gal (Fig. 1A, right lower panel and Fig. 1C), and presented with shortened telomeres (Fig. 1B), suggesting replicative senescence. In addition, the DNA-damaging agent doxorubicin, oxidative stress (application of H_2O_2) and the multi-kinase inhibitor staurosporine induced senescence of young PSC with comparable efficiencies (Fig. 1C). This trigger-mediated senescence occurred within 7 days of treatment of young PSC, and was, like long-term culture, associated with diminished cell proliferation (Fig. 2A). At the relatively low concentration used, neither doxorubicin nor staurosporine (a well-known pro-apoptotic agent) significantly reduced cell survival. H_2O_2 at 150 μM moderately raised the rate of apoptotic cell death from 3.4 ± 1.4% in control cultures to 10.3 ± 5.2% on day 7 (mean values ± S.E.M.; $n = 6$ independent samples; analysed by flow cytometry, applying the sub-G_1-peak method as described in [6]). We also tested the effects of two further established mediators of senescence, mitogenic hyperstimulation with platelet-derived growth factor and expression of

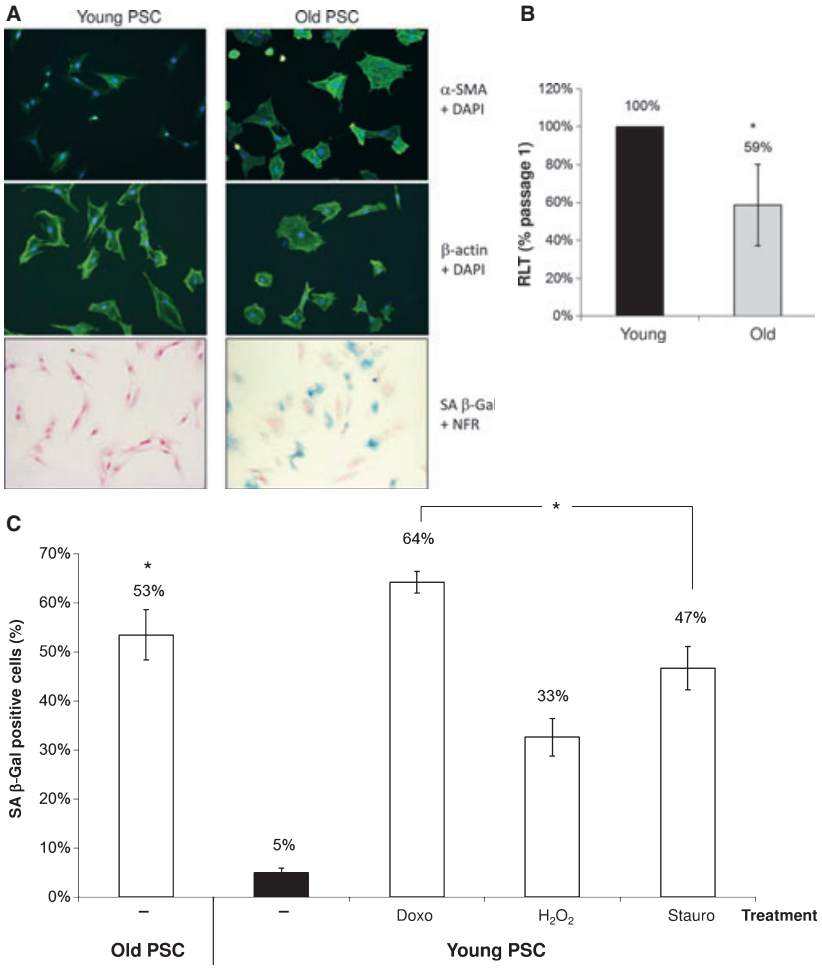

Fig. 1 Senescence of cultured PSC. (**A**) Young and old PSC were subjected to immunofluorescence detection of α-SMA and β-actin (green, stained with AlexaFluor 488; counterstaining: DAPI; upper and middle rows; original magnification ×200), and SA β-Gal staining [counterstaining: nuclear fast red (NFR); lower row; original magnification ×100] followed by light microscopy. (**B**) Relative length of telomeres (RLT) of young and old PSC was determined as described in the Materials and methods section. (**C**) Young PSC were treated with doxorubicin (doxo; 25 ng/ml), H_2O_2 (150 μM) and staurosporine (stauro; 3 nM) for 7 days before SA β-Gal-positive cells were quantified. The number of SA β-Gal-expressing cells is given as percentage of the total cell number. The results in (**B**) and (**C**) are averaged values ± S.E.M. of 5 (in b) and at least 9 (in c) independent experiments. *$P < 0.05$ *versus* untreated young PSC.

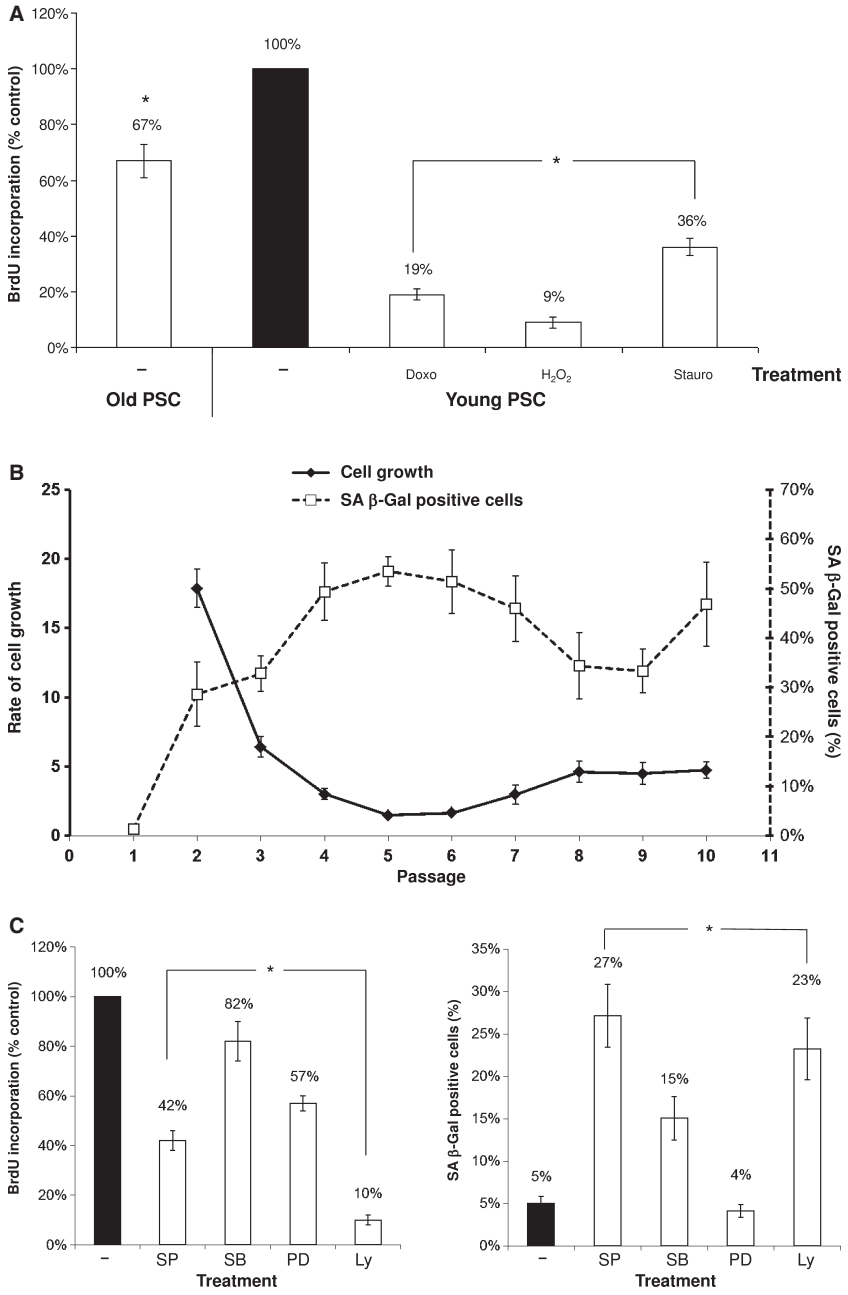

Fig. 2 Cellular ageing and proliferative activity of PSC. (**A**) Young PSC were treated with doxorubicin (doxo; 25 ng/ml), H_2O_2 (150 μM) and staurosporine (stauro; 3 nM) for 24 hrs. Subsequently, young and untreated old PSC were labelled with BrdU overnight. 100% BrdU incorporation corresponds to untreated young PSC. The results are averaged values (±S.E.M.) of at least nine independent samples. $*P < 0.05$ *versus* untreated young PSC. (**B**) Freshly isolated PSC were grown in long-term culture as indicated. Upon re-culture, the cells were counted, re-seeded at constant densities and the ratio of cell densities at harvesting and at seeding was calculated. Furthermore, cells of each passage were cultured on glass coverslips for 1 day. After staining, SA β-Gal-positive cells were quantified and related to the total cell number. The results are averaged values (±S.E.M.) of at least six independent experiments. (**C**) Young PSC were cultured with SP600125 (SP; JNK inhibitor, 20 μM), SB202190 (SB, p38 MAP kinase inhibitor, 20 μM), PD98059 (PD; MEK inhibitor, 25 μM) and LY294002 (LY; PI 3-kinase inhibitor; 10 μM). Left panel: After 24 hrs, the cells were subjected to the quantification of BrdU incorporation. Right panel: SA β-Gal-positive cells were quantified on day 7. BrdU incorporation and SA β-Gal expression data are presented as described above. The results are averaged values (±S.E.M.) of at least nine independent samples. $*P < 0.05$ *versus* untreated young PSC.

the *v-hras* oncogene (induced by transduction of PSC with an adenoviral vector), but did not observe significant increases of senescent cells under the experimental conditions tested (data not shown). When PSC were cultured over 10 passages with one replating per week, SA β-Gal expression and cell proliferation were inversely correlated (Fig. 2B). After 5–6 passages, a plateau level, characterized by roughly 50% SA β-Gal-positive cells and 10% of the original growth rate, was reached and more or less maintained in the course of additional culture.

Mechanisms of PSC senescence *in vitro*

To gain insights into the process of PSC senescence, various signal transduction inhibitors were employed. Inhibition of Jun kinase (JNK), p38 mitogen-activated protein (MAP) kinase, MAP kinase kinase (MEK) and phosphatidylinositol (PI) 3-kinase with SP600125, SB202190, PD98059 and LY294002, respectively, was associated with a significant reduction of cell proliferation (Fig. 2C). Blockade of JNK, p38 MAP kinase and PI 3-kinase lead

to a significant increase of SA β-Gal-positive cells, whereas MEK inhibition was associated with a small decrease of senescent PSC.

We next studied gene expression profiles of senescent and non-senescent PSC. Based on pilot studies, a panel of potential senescence-associated genes was selected for additional analysis. Figure 3A reveals that doxorubicin, H_2O_2 and staurosporine-induced senescence was associated with characteristic expression changes: Young PSC treated with any of the triggers expressed higher mRNA levels of IL-6, CDKN1A/p21 and the p53 inhibitor Mdm2, but lower levels of α-SMA than untreated PSC. With respect to p53 expression, the triggers displayed diverse effects (doxorubicin: inhibition, H_2O_2: no effect, staurosporine: induction). When cellular senescence was induced by long-term culture, changes of gene expression were observed that mimicked the effects of doxorubicin (Fig. 3B, upper panel). The only exception refers to α-SMA which was found at higher levels in old than in young PSC. However, as also shown in Fig. 3B (lower panel), α-SMA expression in old PSC (passage 5 and beyond) was below the maximum, which was reached around passage 3. With respect to IL-6, mRNA expression data were also confirmed at the protein level (Fig. 3C). Together, these data suggest large overlaps in the gene expression profiles of senescent PSC, independent of the mechanism that induced cellular ageing.

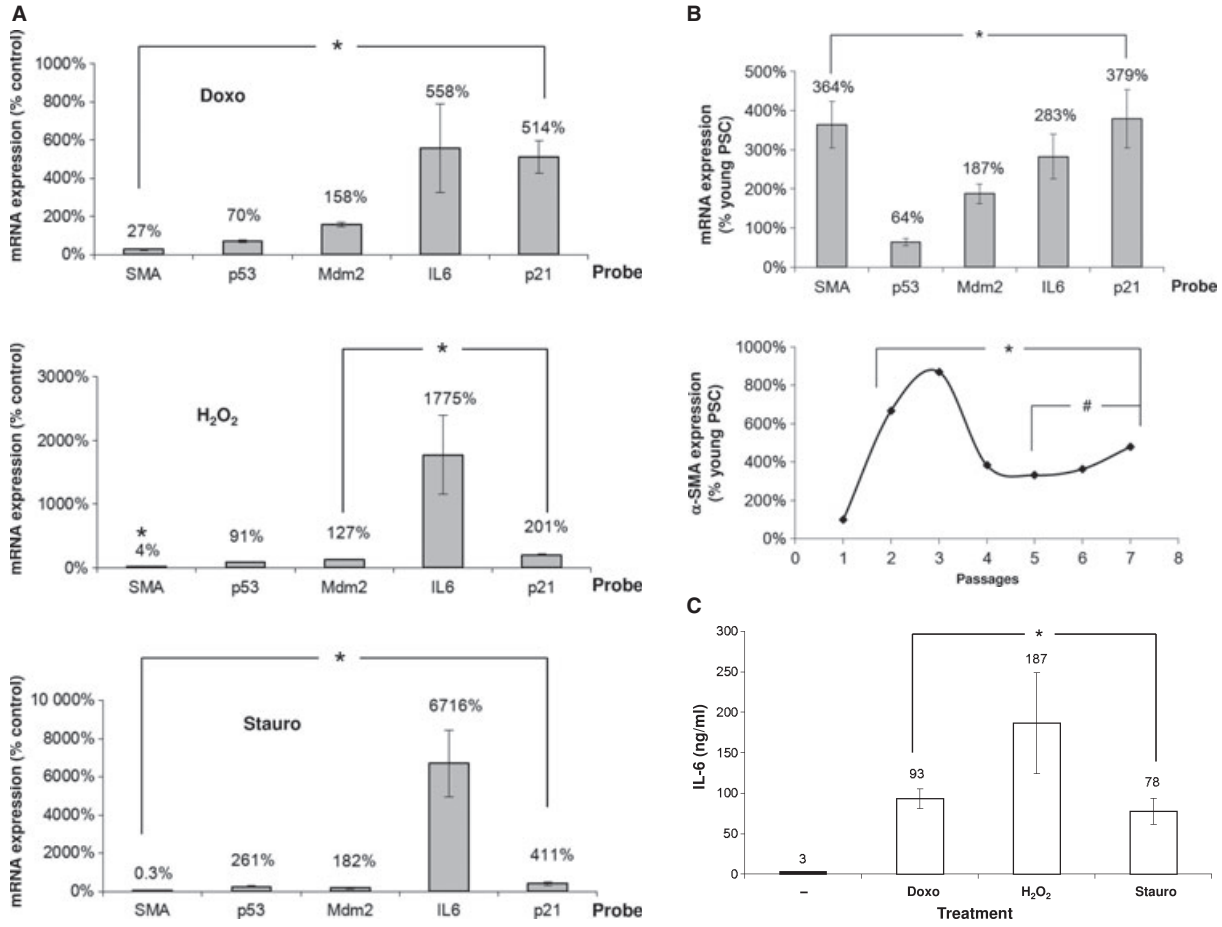

Fig. 3 Gene expression profile of senescent PSC. (**A**) Young PSC were treated for 7 days with doxorubicin (doxo; 25 ng/ml; upper panel), H_2O_2 (150 μM; middle panel) and staurosporine (stauro; 3 nM; lower panel) to induce senescence. The mRNA expression of α-SMA (SMA), p53, Mdm2, IL-6, CDKN1A/p21 and the housekeeping gene HPRT was analysed by real-time PCR, and relative amounts of target mRNA were determined. (**B**) Upper panel: Untreated young and old PSC were subjected to gene expression analysis as described in (**A**). Lower panel: Time course of α-SMA mRNA expression in untreated PSC. The first time-point refers to young PSC, the following ones to cells of consecutive passages. (**A**) and (**B**): One hundred per cent mRNA expression of each gene corresponds to untreated young PSC. Data of at least six independent experiment were used to calculate mean values and S.E.M. $*P < 0.05$ *versus* untreated young PSC, $^{\#}P < 0.05$ *versus* passage 3. (**C**) IL-6 protein levels in supernatants of young PSC, treated for 7 days as indicated, were measured as described in the Materials and methods section. The results are averaged values (±S.E.M.) of at least five independent experiments. $*P < 0.05$ *versus* untreated young PSC.

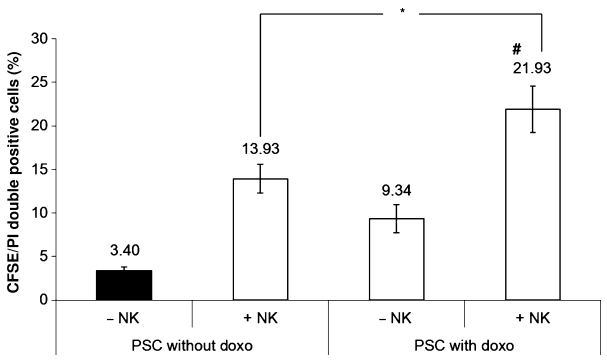

Fig. 4 Effects of NK cells on activated or senescent PSC. PSC of passage 1 were exposed to doxorubicin (doxo; 25 ng/ml) for 7 days as indicated, or left untreated. After staining with CFSE, PSC were trypsinized and recultured together with NK cells at a ratio of 1:20 as indicated. After 16 h, the cells were harvested, labelled with PI and subjected to FACS analysis. CFSE and PI double-positive (dead) PSC are expressed as percentage of all CFSE-labelled cells. The results are averaged values (±S.E.M.) of 11 independent experiments. $*P < 0.05$ *versus* PSC cultured without doxorubicin and NK cells, $\#P < 0.05$ *versus* PSC cultured without doxorubicin, with NK cells.

Senescent PSC are highly susceptible to immune cell-mediated cytotoxicity

Untreated PSC displayed an approximately fourfold increased rate of cell death upon coculture with NK cells (Fig. 4). Treatment with doxorubicin in the absence of NK cells also somewhat increased the number of PI-positive cells, probably due to a reduced resistance of these cells to the stress of trypsination and reculture. By far the highest rate of lysis was observed when doxorubicin-pre-treated PSC were cocultured with NK cells. Similar data were obtained when NK cells were replaced by unpurified spleen cells (data not shown). As typically less than 5% of all splenocytes were NK cells, these data suggest that immune cells other than NK cells may also exert cytolytic effects on cultured, in particular senescent PSC.

Involvement of cellular senescence in pancreatic wound healing

Application of DBTC at 6–8 mg/kg causes in rats a pancreatic inflammation which resembles key features of human chronic pancreatitis, including infiltration with immune cells and fibrosis [12, 15]. To study relationships between the course of inflammation, stellate/immune cell activation and cellular senescence, a series of experiments with two different doses of DBTC (6 and 8 mg/kg respectively) and several time-points after DBTC application (1, 2, 4 and 8 weeks) was initiated.

Figure 5 shows exemplary histopathological changes 1 week after application of DBTC at 8 mg/kg: H&E staining (A) revealed a severe damage to the pancreatic parenchyma, an infiltration with inflammatory cells and a beginning periductal and interstitial fibrosis. In accordance with published data [17], predominantly not only CD4 but also CD8-positive lymphocytes were detected (B, D). Furthermore, cells expressing the rat NK cell marker CD161 were found in significant numbers (E). The figure also indicates that many cells with a periacinar distribution stained positive for α-SMA (C) and desmin (F), suggesting activation of stellate cells. At later stages of the disease, the pattern of α-SMA staining changed from a scattered, periacinar to a more extended, predominantly periductal one (see Fig. 6B for an example).

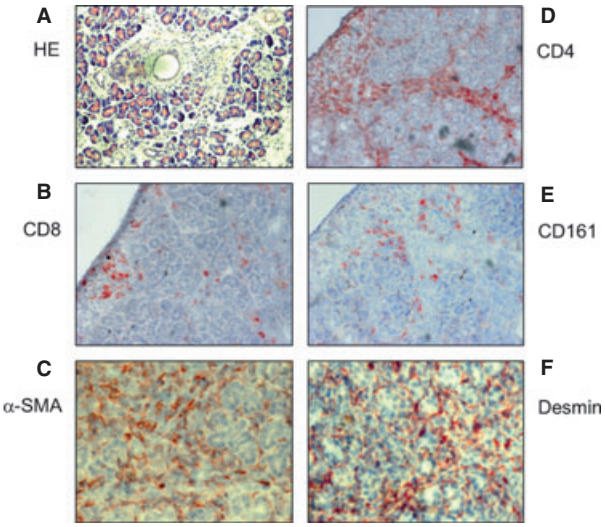

Fig. 5 Histological characteristics of DBTC-induced pancreatitis. Pancreatitis was induced by the injection of DBTC (8 mg/kg). All microphotographs correspond to pancreatic sections of a rat killed on day 7 after DBTC application, and are representative of at least 10 animals analysed. (**A**) H&E staining of paraffin-embedded tissue reveals typical histology of the disease, including acinar cell damage, ductal changes, periductal and interstitial fibrosis and inflammatory cell infiltrates. (**B**–**F**) Cryostat tissue sections were used to detect CD4, CD8 and CD161-positive lymphocytes as well as cells expressing the PSC markers α-SMA and desmin, employing specific antibodies and the APAAP technique. (**A**, **B**, **D**, **E**) original magnification ×100, (**C** and **F**): ×200. The lymphocyte stainings were performed on serial sections of the tissue.

Figure 6 shows, for a sample obtained 2 weeks after application of DBTC at 8 mg/kg, that large areas of the parenchyma also stained positive for SA β-Gal (A). As suggested by the results of α-SMA staining, these regions largely overlapped with areas of periductal fibrosis (B). In the same regions, also dense infiltrates of immune cells were observed (C, exemplary showing CD4 staining). A close proximity of α-SMA-expressing cells and immune cells (CD4 and CD161-positive respectively) was also confirmed by immunofluorescence studies (Fig. S1). Subsequently, a detailed quantitative evaluation of various histological and immunohistochemical parameters was performed (Fig. 7). Because we did not detect differences between the two early time-points after DBTC injection, these data are presented as one group (week 1–2). As expected, the lower dose of DBTC was associated with less severe pancreatitis. Thus, the overall assessment of pancreatic histopathology and a semi-quantitative evaluation of

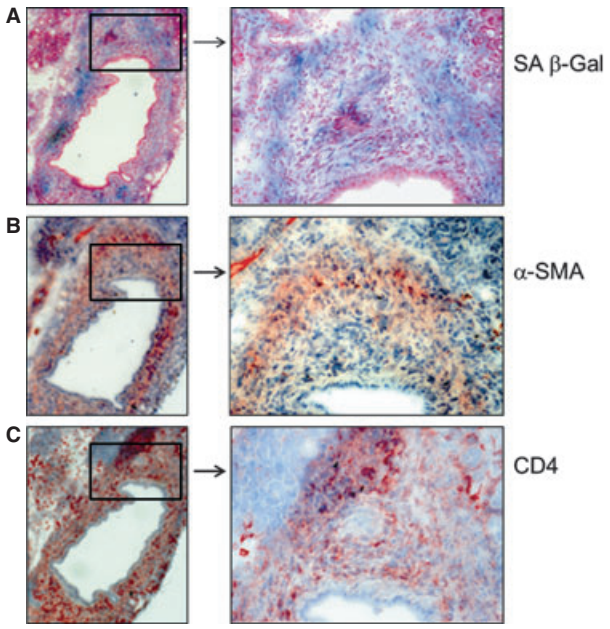

Fig. 6 Colocalization of senescence, inflammation and fibrosis markers. Pancreatitis was induced by the injection of DBTC (8 mg/kg). The microphotographs correspond to serial pancreatic cryostat sections of a rat 2 weeks after DBTC injection, and are typical of at least 10 animals analysed. (**A**) Senescent cells were detected by SA β-Gal staining. (**B** and **C**) Cells expressing α-SMA and CD4-positive lymphocytes were stained with specific antibodies, using the APAAP technique. Left panels: original magnification ×25, right panels: ×100.

fibrosis yielded higher scores in the 8 mg/kg group at any time point (A, B). Furthermore, lower numbers of α-SMA-expressing cells, CD4- and CD161-positive lymphocytes were detected (D, E, F) in the 6 mg/kg group. None of the parameters studied (except of α-SMA in the 6 mg/kg DBTC group) returned to baseline levels until week 8, suggesting a chronic course of the disease. With few exceptions, peak values of these scores and cell counts were detected at the earliest time-point, otherwise in week 4. Similar time courses were observed for infiltration of pancreatic tissue with CD8-positive lymphocytes, granulocytes and macrophages (data not shown). SA β-Gal-positive regions (C) reached their maximum extension also early in the course of the disease, peaking in week 1–2 (8 mg/kg group) and week 4 (6 mg/kg group) respectively. The healthy organ was virtually free of SA β-Gal-expressing cells. In conclusion, processes of tissue damage, repair and cell senescence proceeded in parallel and in a coupled (rather than consecutive) fashion.

To gain additional pathophysiological insights, rats were depleted of NK cells prior to the induction of pancreatitis. Figure S2 shows that an anti-CD161 treatment caused an almost complete elimination of NK cells in the blood and a reduction by roughly two thirds in the inflamed pancreas. However, this was not associated with significant changes of disease severity, stellate cell activation, fibrosis, infiltration with other immune cells and extension of SA β-Gal-positive regions (data not shown).

Discussion

Cellular senescence represents a programme that is activated in response to various types of stress, such as telomere uncapping, DNA damage, reactive oxygen species, oncogene activity in normal cells, lack of growth factors and improper cell contacts [18]. Upon activation of the senescence programme, cells cease to divide and undergo characteristic morphological and metabolic changes. Although it is generally accepted that cellular senescence imposes a barrier to tumourigenesis [11, 18], its functional contribution to non-cancer pathologies is poorly understood. Furthermore, the molecular mechanisms involved in the induction and maintenance of senescence, and their cell type-specific differences, are not fully elucidated yet.

In this study, we have focused on the contribution of senescence processes to pancreatic inflammation and wound healing, paying particular attention to pancreatic stellate cells. PSC are considered a principal cell type in pancreatic tissue repair, as they are the main source of extracellular matrix proteins in the inflamed organ [1, 2]. PSC have also been proposed to display some features of progenitor/stem cells, and may play a role in pancreatic regeneration beyond fibrogenesis [19, 20]. Persistent activation of PSC, on the other hand, can result in organ fibrosis and contribute to the progression of both chronic pancreatitis and pancreatic cancer [1, 2]. The mechanisms controlling pancreatic wound healing are, therefore, of potential clinical interest.

Our *in vitro* studies showed that rat PSC after 5–6 passages reached a plateau state with roughly 50% senescent cells (assessed by SA β-Gal expression). Three different stressors, doxorubicin, H_2O_2 and staurosporine, displayed quantitatively similar effects, but did also not induce senescence of all PSC. Together, these data support the conclusion that PSC, like HSC [10], are susceptible to the induction of replicative and stressor-induced senescence. We also hypothesize that long-term culture may select a sub-population of PSC with the capability of keeping the number of senescent cells at a nearly constant level, possibly through a potential of prolonged self-renewal. In this context, it is interesting to note that a recent study has identified a pancreatic stellate cell population with properties of progenitor cells [19]. The regenerative capacity of PSC, therefore, deserves additional investigation.

In accompanying studies, we asked if the ageing process of PSC in culture may also depend on the age of the rats. We found that PSC from 18-month-old rats proliferated at a lower rate and displayed a somewhat increased rate of SA β-Gal-positive cells early after isolation, while later passages of PSC from 3- and 18-month-old rats were virtually indistinguishable (Fig. S3). Furthermore, after doxorubicin treatment more PSC from old than from young rats became senescent. These data suggest age of the individual as a modifying factor of cellular senescence in the context of PSC activation.

Studies on gene expression profiles of senescent PSC and transduction of senescence signals revealed both similarities with other cell types and peculiar aspects. Specifically, increased secretion of IL-6 resembles the senescence-associated secretory phenotype of other types of senescent cells, including HSC [12]. The cell cycle inhibitor CDKN1A/p21, a downstream target of p53, has been implicated in the induction of senescence in various types of cells [10, 18, 21]. In overexpression studies, we observed that increased levels of CDKN1A/p21 not only accompany the senescence process (as shown

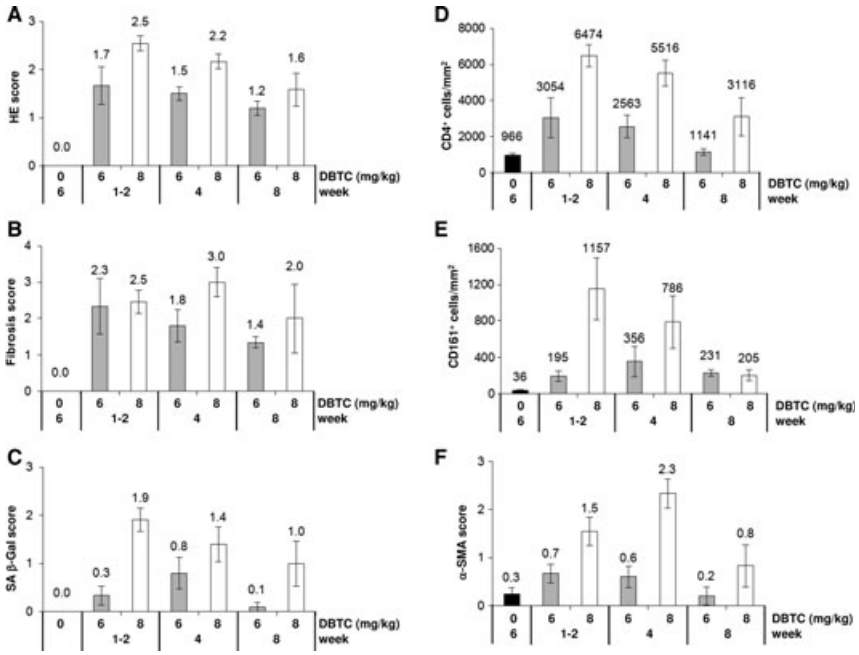

Fig. 7 Semi-quantitative and quantitative assessment of histopathological changes in rats with DBTC-induced pancreatitis. To induce mild or more severe chronic pancreatitis, DBTC was injected at 6 and 8 mg/kg, respectively. At the indicated time points, the rats were killed and pancreatic tissue subjected to histopathological evaluation. (**A**) Applying a semi-quantitative score from 0 to 3, an overall assessment of disease severity was conducted as described in the Materials and methods section, using H&E stained samples. (**B**) After H&E staining, extension of fibrosis was judged on a scale from 0 to 6 points (up to 3 points for most severe periductal and interstitial fibrosis respectively). (**C**) Extension of areas covered with SA β-Gal-positive cells was evaluated on a scale from 0 to 3. (**D**–**F**) After APAAP staining with specific antibodies, α-SMA expression was assessed using a scale from 0 to 3 (lower panel). CD4 and CD161-positive cells (upper and middle panel) were counted, employing an ocular grid, at a magnification of 400×. All results are averaged values (±S.E.M.) of at least five rats per experimental group.

herein), but play a direct role in its initiation/progression in PSC (B. Fitzner and R. Jaster, unpublished data). Somewhat surprising, the mRNA level of p53 was found to be diminished by doxorubicin treatment and long-term culture, and one of its inhibitor Mdm2 [22] increased in all senescent cells. Given that p53 not only plays a key role in the induction of senescence in HSC but may also exert paradoxical effects in some cells under special circumstances [10, 18, 23], this observation requires additional investigation. Interestingly, senescent PSC displayed lower levels of α-SMA mRNA than activated cells of earlier passages. Along with the reduced proliferation rate, this feature of senescent PSC resembles to some degree the phenotype of quiescent cells and distinguishes them from fully activated young PSC.

We found that blockade of p38 MAP kinase, JNK, but not MEK was associated with increased rates of SA β-Gal-positive PSC. With respect to the roles of p38 MAP kinase and MEK, our data are in agreement with previously published data [24, 25]. In contrast, inhibition of JNK has previously been suggested to interfere with the senescence process [24, 26], and hyperactivation of PI 3-kinase signalling promotes ageing in some types of cells [27]. If these differences are cell type-dependent, remains to be investigated further. At this stage, our data suggest that (i) inhibition of proliferation alone is insufficient to induce senescence of PSC, and (ii) senescence of PSC is regulated by several primarily independent signal transduction pathways.

To address the role of cellular senescence in the context of pancreatic inflammation and fibrosis *in vivo*, the model of DBTC-induced chronic pancreatitis in rats was applied. The data suggest cellular senescence as a common phenomenon in the inflamed organ, which is directly correlated with the severity of the inflammatory process. Senescent cells were present early in the course of inflammation already and largely disappeared when inflammation attenuated. To gain further insights into the coupling of these processes, follow-up studies with a higher resolution time course are required.

The results of our colocalization studies raised the question if senescent PSC, like HSC in liver fibrosis [10], might be targeted by immune cells, specifically NK cells, to undergo cell death, thereby terminating pancreatic fibrogenesis. In coculture experiments, both splenocytes and purified NK cells exerted cytolytic effects on activated PSC. Senescence of PSC was found to be not essential for immune cell-mediated killing of activated PSC, but increased the efficiency of cytolysis. The results, however, did not reveal a specific role of NK cells in this process, because unpurified spleen cells displayed a similar effect. Moreover, when rats were depleted of NK cells, severity of DBTC-pancreatitis and specifically fibrosis were not affected. In this regard, our findings differ from findings in the liver, where NK cells have been suggested to play a pivotal role in the resolution of fibrosis [10]. A possible explanation is provided by our observation that NK

cells, although present in large numbers in the inflamed pancreas, still represent a minority of all infiltrating lymphocytes only. As shown herein, CD4-positive T cells are the dominant fraction of lymphocytes at least during the first weeks of chronic DBTC-pancreatitis. These T cells and other immune cells are a rich source of various cytokines with established activating effects on quiescent PSC [28, 29]. Based on our results, we now propose a model in which lymphocytes play a dual-specific role in the course of pancreatic inflammation, triggering both the initiation of wound healing (by activating PSC) and its termination (by killing senescent stellate cells). The specific contribution of individual subsets of lymphocytes should be addressed further.

In conclusion, the results of this study suggest that inflammation, PSC activation and cellular senescence are timely coupled processes and take place in the same microenvironment of the inflamed pancreas. The data are in agreement with the hypothesis that cellular senescence represents an integral component of pancreatic wound healing.

Acknowledgements

We gratefully acknowledge the excellent technical assistance of Mrs Katja Bergmann and Mrs Katrin Sievert-Küchenmeister. This work was supported by a grant from the Deutsche Forschungsgemeinschaft (to RJ).

Conflict of interest

All authors declare to have no conflict of interest.

Supporting information

Additional Supporting Information may be found in the online version of this article:

Fig. S1 Close proximity of lymphocytes and stellate cells in inflamed pancreatic tissue.

Fig. S2 Efficient reduction of rat NK cells by anti-CD161 treatment.

Fig. S3 Rates of DNA synthesis and expression of SA β-Gal in PSC isolated from rats of different age.

Please note: Wiley-Blackwell are not responsible for the content or functionality of any supporting materials supplied by the authors. Any queries (other than missing material) should be directed to the corresponding author for the article.

References

1. **Erkan M, Adler G, Apte MV, *et al.*** StellaTUM: current consensus and discussion on pancreatic stellate cell research. *Gut.* 2012; 61: 172–8.
2. **Jaster R, Emmrich J.** Crucial role of fibrogenesis in pancreatic diseases. *Best Pract Res Clin Gastroenterol.* 2008; 22: 17–29.
3. **McCarroll JA, Phillips PA, Santucci N, *et al.*** Vitamin A inhibits pancreatic stellate cell activation: implications for treatment of pancreatic fibrosis. *Gut.* 2006; 55: 79–89.
4. **Froeling FE, Feig C, Chelala C, *et al.*** Retinoic acid-induced pancreatic stellate cell quiescence reduces paracrine Wnt-β-catenin signaling to slow tumour progression. *Gastroenterology.* 2011; 141: 1486–97, 97.e1–14.
5. **Klonowski-Stumpe H, Fischer R, Reinehr R, *et al.*** Apoptosis in activated rat pancreatic stellate cells. *Am J Physiol Gastrointest Liver Physiol.* 2002; 283: G819–26.
6. **Jaster R, Lichte P, Fitzner B, *et al.*** Peroxisome proliferator-activated receptor γ overexpression inhibits pro-fibrogenic activities of immortalized rat pancreatic stellate cells. *J Cell Mol Med.* 2005; 3: 670–82.
7. **Rickmann M, Vaquero EC, Malagelada JR, *et al.*** Tocotrienols induce apoptosis and autophagy in rat pancreatic stellate cells through the mitochondrial death pathway. *Gastroenterology.* 2007; 132: 2518–32.
8. **Manapov F, Muller P, Rychly J.** Translocation of p21(Cip1/WAF1) from the nucleus to the cytoplasm correlates with pancreatic myofibroblast to fibroblast cell conversion. *Gut.* 2005; 54: 814–22.
9. **Krizhanovsky V, Yon M, Dickins RA, *et al.*** Senescence of activated stellate cells limits liver fibrosis. *Cell.* 2008; 134: 657–67.
10. **Krizhanovsky V, Xue W, Zender L, *et al.*** Implications of cellular senescence in tissue damage response, tumour suppression, and stem cell biology. *Cold Spring Harb Symp Quant Biol.* 2008; 73: 513–22.
11. **Campisi J, d'Adda di Fagagna F.** Cellular senescence: when bad things happen to good cells. *Nat Rev Mol Cell Biol.* 2007; 8: 729–40.
12. **Sparmann G, Merkord J, Jäschke A, *et al.*** Pancreatic fibrosis in experimental pancreatitis induced by dibutyltin dichloride. *Gastroenterology.* 1997; 112: 1664–72.
13. **Jaster R, Sparmann G, Emmrich J, *et al.*** Extracellular signal-regulated kinases are key mediators of mitogenic signals in rat pancreatic stellate cells. *Gut.* 2002; 51: 579–84.
14. **Brock P, Sparmann G, Ritter T, *et al.*** Interleukin-4 gene transfer into rat pancreas by recombinant adenovirus. *Scand J Gastroenterol.* 2005; 40: 1109–17.
15. **Merkord J, Jonas L, Weber H, *et al.*** Acute interstitial pancreatitis in rats induced by dibutyltin dichloride (DBTC): pathogenesis and natural course of lesions. *Pancreas.* 1997; 15: 392–401.
16. **Fitzner B, Brock P, Holzhüter SA, *et al.*** Synergistic growth inhibitory effects of the dual endothelin-1 receptor antagonist bosentan on pancreatic stellate and cancer cells. *Digest Dis Sci.* 2009; 54: 309–20.
17. **Sparmann G, Behrend S, Merkord J, *et al.*** Cytokine mRNA levels and lymphocyte infiltration in pancreatic tissue during experimental chronic pancreatitis induced by dibutyltin dichloride. *Dig Dis Sci.* 2001; 46: 1647–56.
18. **Ben-Porath I, Weinberg RA.** The signals and pathways activating cellular senescence. *Int J Biochem Cell Biol.* 2005; 37: 961–76.
19. **Docherty K.** Pancreatic stellate cells can form new beta-like cells. *Biochem J.* 2009; 421: e1–4.
20. **Mato E, Lucas M, Petriz J, *et al.*** Identification of a pancreatic stellate cell population with properties of progenitor cells: new role for stellate cells in the pancreas. *Biochem J.* 2009; 421: 181–91.
21. **Dotto GP.** p21(WAF1/Cip1): more than a break to the cell cycle?. *Biochim Biophys Acta.* 2000; 1471: M43–56.
22. **Wang Z, Li B.** Mdm2 links genotoxic stress and metabolism to p53. *Protein Cell.* 2010; 1: 1063–72.

23. **Demidenko ZN, Korotchkina LG, Gudkov AV, *et al.*** Paradoxical suppression of cellular senescence by p53. *Proc Natl Acad Sci USA.* 2010; 107: 9660–4.
24. **Spallarossa P, Altieri P, Barisione C, *et al.*** p38 MAPK and JNK antagonistically control senescence and cytoplasmic p16INK4A expression in doxorubicin-treated endothelial progenitor cells. *PLoS ONE.* 2010; 5: e15583.
25. **Yang M, Zhang M, Chen J, *et al.*** Angiopoietin-1 inhibits mouse glomerular endothelial cell senescence *via* Tie2 receptor-modulated ERK1/2 signaling. *Am J Nephrol.* 2010; 31: 490–500.
26. **Lee JJ, Lee JH, Ko YG, *et al.*** Prevention of premature senescence requires JNK regulation of Bcl-2 and reactive oxygen species. *Oncogene.* 2010; 29: 561–75.
27. **Astle MV, Hannan KM, Ng PY, *et al.*** AKT induces senescence in human cells *via* mTORC1 and p53 in the absence of DNA damage: implications for targeting mTOR during malignancy. *Oncogene.* 2012; 31: 1949–62.
28. **Michalski CW, Gorbachevski A, Erkan M, *et al.*** Mononuclear cells modulate the activity of pancreatic stellate cells which in turn promote fibrosis and inflammation in chronic pancreatitis. *J Transl Med.* 2007; 5: 63.
29. **Sparmann G, Glass A, Brock P, *et al.*** Inhibition of lymphocyte apoptosis by pancreatic stellate cells: impact of interleukin-15. *Am J Physiol Gastrointest Liver Physiol.* 2005; 289: G842–51.